# Computer Simulation of the Liquid Crystal Formation in a Semi-Flexible Polymer System

*Anatoly A. Darinskii*[a], *Igor M. Neelov*[a,b], *Anna Zarembo*[b,*], *Nikolai K. Balabaev*[c], *Franciska Sundholm*[b], *Kurt Binder*[d]

[a] Institute of Macromolecular Compounds, Bolshoi pr.31, 199004 St.-Petersburg, Russia
[b] University of Helsinki, P.O.Box 55, FIN-00014 Helsinki, Finland
[c] Institute of Mathematical Problems of Biology, 142292 Pushchino, Russia
[d] J.-Gutenberg University, Staudingerweg 10, D-55099, Mainz, Germany

**Summary:** Molecular dynamic simulations are reported for system of semi-flexible linear rod-like molecules. The molecules are composed of $N_C$ tangent soft spheres, connected by elastic springs. Rigidity is introduced by additional springs between all pairs of spheres along the molecule. The formation of only a nematic LC phase is shown for all systems with $N_C = 8$ and different flexibility. The effect of flexibility on the order parameter and the volume fraction at the LC phase transition is compared with theoretical predictions by Khokhlov-Semenov and with available simulation data. The dependence of the anisotropy of diffusion on chain flexibility in LC phase was studied. The polymer brushes consisting of flexible and semi-flexible (composed of linear rod-like segments) chains were simulated at different grafting densities. Height of brush, order parameter, distribution of density and chain ends in brush were obtained in both cases and compared with theoretical predictions.

**Keywords:** Liquid- crystalline polymers; Polymer brushes; Simulations

## Introduction

It is well known that solutions of molecules with the sufficient shape anisotropy are able to form a lyotropic LC phase at definite concentrations. The theory of LC formation for thin rigid rods was developed by Onsager[1] on the base of the second-order virial expansion. Many real LC systems consist of semi-flexible molecules. In particular the flexibility plays an important role in the statistical physics of liquid crystalline polymers. [2,3] Semiflexible LC polymers show a wide variety of phase behaviour and play an important role in biology and materials science.[4] Khokhlov and Semenov [5, 6] have generalized the Onsager's approach for semiflexible molecules on the base of the persistent model. The ideas by Khokhlov and Semenov were developed later by several authors (see review [3]). A slightly different approach was used recently in [7]. All theories predict a

CCC 1022-1360/00/$ 17,50+.50/0

LC transition for sufficiently long molecules with definite flexibility.

Another approach to the theoretical study of LC transitions in polymers consists of computer simulations. The most used are models of a single rigid anisotropic mesogene , such as hard ellipsoids and spherocylinders[8] or particles with soft anisotropic Gay-Berne potential[9]. The review of the results in this field has been given by Allen[10]. For the simulation of semi-flexible molecules the models consisting of the many particles are necessary. Such models were used by Allen and Wilson[11], Dijkstra and Frenkel [12] ,Yethiraj and Fynewever[13] and Kolb[14]. If the flexibility of molecules was below some value the transition from isotropic to LC state was observed for all models at some density. This density decreased with increasing the length of molecule or decreasing its flexibility.

In our recent MD simulation[15] a system of semi-flexible linear molecules, which resembles both that of Allen and Wilson and that of Kolb was studied. In [15] the three systems with the same flexibility but with the different numbers of particles $N_c$ =6, 7, 8 in each molecule were simulated. The formation of the nematic LC phase was observed only for $N_c$ =8. In the present work we study the effect of the varying flexibility on LC transition and diffusion for $N_c$ =8.

We also use the similar linear rod-like segments with $N_c$=5 connected into linear chains for simulation of the semi-flexible polymer brushes.

## Model and Method of Simulation

For the simulation of the LC transition in a concentrated solution of anisotropic mo;ecules we use as a model a semiflexible rod-like linear molecule, consisting of $N_c$ Lennard-Jones (LJ) particles. All particles in the system interact according to shifted and truncated LJ 6-12 potential $U_{LJ}$, which corresponds to pure repulsive interactions between the particles in the system:

$$U_{LJ}=4\varepsilon((\sigma/r)^{12}-(\sigma/r)^{6})+\varepsilon \quad \text{if } r\leq 2^{1/6} \text{ and } U=0 \text{ if } r>2^{1/6}, \qquad (1)$$

where $r$ is the distance between the particles, $2^{1/6}$- the radius of truncation, $\sigma$ and $\varepsilon$ are equal to $1$.

Rigidity of the molecule is introduced by Frenkel's springs between all particles along the chain. The potential of the spring between $i$ -th and $s$-th particles of linear molecule is given by

$$U_{si}=\frac{K_{si}}{2}(|r_i-r_s|-(i-s)l_0)^2 \qquad s=1, N_c-1,\ i=s+1, N_c \qquad (2)$$

where $l_o$ is the equilibrium bond length assumed $l_o=\sigma$ and $s$ is the number of particles in chain.

We consider the model in which all springs (including the bond length one) have the same elasticity constant $K_s$. The layout of the model is shown in Figure 1. In our previous work [15] we studied only the case of the moderate spring elasticity $K_s$ =50 for different $N_c$. In the present work we vary $K_s$ at constant chain length $N_c$ =8. Three systems with the spring elasticity $K_s$ =50, 100 and 500 are considered.

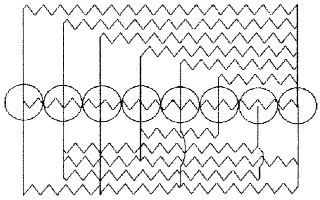

Figure 1. Layout of the model mesogen with $N_c$=8.

The simulation was performed by the molecular dynamics method using the Verlet algorithm[16] for the numerical integration of equations of motion. The simulated systems contained $N_m$ =1536 molecules in the simulation box. The reduced units for time $\tau = \sigma (m / \varepsilon)^{1/2}$ and length $\sigma$ were used as usual. The integration step $\Delta t$=0.004 was selected. All calculations were performed at the same temperature $T=0.5/k_B$ where $k_B$ is the Boltzman constant.

In the initial conformation all spheres were on a simple cubic lattice with 48*16*16 sites. A regular completely ordered array of 6 layers of linear molecules (8 spheres in each) with number density $\rho = N_m N_c / V$=1 was used. Molecules were aligned parallel to the long axis OZ of the simulation cell. In perpendicular (X and Y) directions molecules initially form the square lattice of 16*16. This size is enough to avoid the intersections of images of molecules in neighbouring cells. To obtain systems with different densities the periodical boundary conditions were applied and the systems were equilibrated at constant temperature and pressure (NPT ensemble) by Berendsen method [17]. The equilibrium state was considered being achieved after the density and order parameter became stable on a sufficiently long part of the trajectory. After this equilibration the static and dynamical characteristics of the systems were calculated using NVT ensemble (the constant temperature and volume). The lengths of the runs were about $10^5$ time steps.

For the simulation of polymer brushes we simulated a system of n=100 chains anchored by one end to the inpenetrable plane at different grafting densities *a=n/A (A* is the plane area). Grafting points form the square lattice (10*10) in Z=0 plane. Periodic boundary conditions in two (X and Y) dimensions were imposed. In the semi-flexible brush every chain consisted of 12 freely-jointed mesogens similar to that shown on Figure 1 but with $N_c$ =5 and $K_s$ =50. In the flexible brush the chains with the same contour lengths were used but all elastic potential between non-neighbouring spheres were removed. Brushes with chain completely stretched in the direction Z normal to the plane were used as initial configurations. The simulation time was from $10^6$ to $10^7$ time steps.

## Results and Discussion

### Solution of Semi-Flexible Molecules. Static Characteristics

The order parameter $S$ and direction of orientation was calculated from the ordering tensor

$$Q_{\alpha\beta}^{aa} = \frac{1}{N_m}\sum_{j=1}^{N_m}\frac{3}{2}a_{j\alpha}a_{j\beta} - \frac{1}{2}\delta_{\alpha\beta} \quad \alpha,\ \beta = x, y, z \qquad (3)$$

Dependences of the order parameter $S$ on the density for systems considered are shown in Figure 2. The curves shift to larger values of density with the increase of flexibility. Also the data for the chains with $N_c$ =8 obtained by Kolb [14] for $l_p$ =1000 and Yethiraj and Fynewever[13] for infinite $l_p$ are plotted.

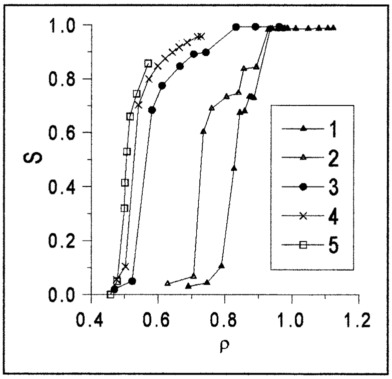

Figure.2 Order parameter dependence of density: 1- $K_s$ =50, 2 - $K_s$=100, 3 - $K_s$=500, 4- ref.[14] , 5- ref. [13].

Data show the existence of an intermediate stable state with the order parameter $S$=0.6-0.9 between crystalline and isotropic states. The nature of this intermediate phase was studied by calculating a number of structural features: the distribution of particles along the axes of regularity and in the perpendicular direction, the binary distribution function of the centres of mass, the radial binary distribution function of the centres of

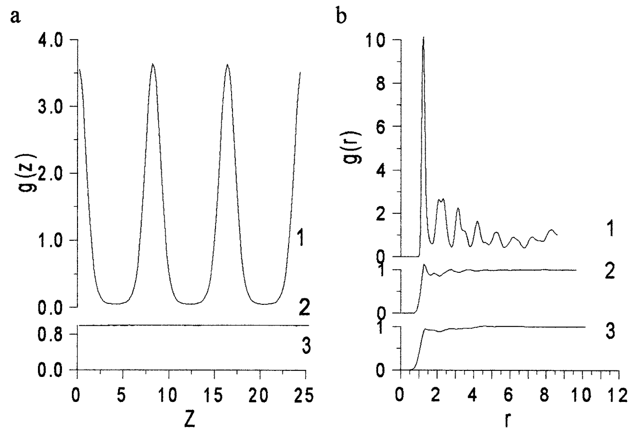

Figure 3. Binary distribution function g (z) along OZ axis (a) and radial binary distribution function g(r) of the centres of mass (b): 1- crystal , 2- nematic , 3-isotropic phase.

mass and pairwise orientational correlation function were calculated for all phases obtained in the simulation. Examples of these characteristics for $K_s$ =500 are given in Figure 3. It follows from the analysis of these data for all systems considered the intermediate phase corresponds to the nematic one. The snapshots (Figure 4) confirm this conclusion.

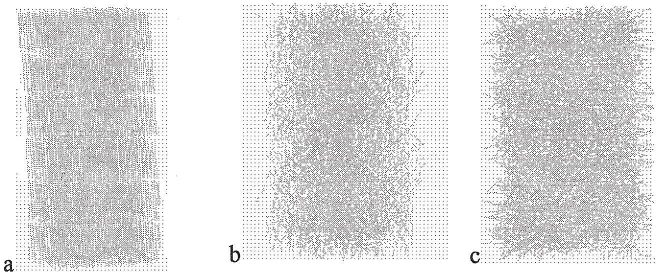

Figure 4. Typical snapshots of three states of the simulated systems: a) completely ordered state (isometry); b) LC state (XZ plane); c) isotropic state (XZ plane)

We have not observed the formation of the smectic even in case of the most rigid chains. The position of the transition from the crystalline to the nematic state was determined from dependence of $S(\rho)$, as a region where $S$ starts to drop abruptly. It is shifted to smaller densities as Ks increases.

The pressure dependences on the density $P(\rho)$ for systems considered are shown in Figure 5. The curves for more flexible systems are shifted to smaller densities. These results are in a qualitative agreement with the results obtained by Hentschke[19] for the density dependence of the osmotic pressure of the solution of wormlike chains.

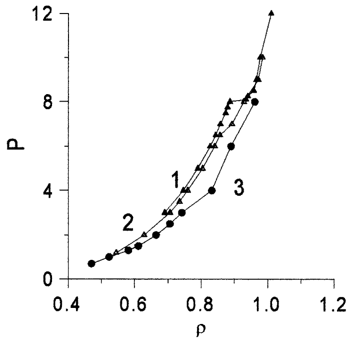

Figure 5. Pressure dependence on density for systems: 1- $K_s$ =50, 2 - $K_s$=100, 3 - $K_s$=500.

Theories of LC transitions in polymers connect the jump of the order parameter $\Delta S$ and volume fractions of isotropic $\Phi_i$ and nematic phases $\Phi_n$ at the I-N transition with ratio $L$ to $l_p$.. Khokhlov – Semenov[2] (KS) theory for a hard wormlike cylinder model predicts for the case $L / l_p \ll 1$:

$$\Delta S = 0.847 - 1.487 L / l_p \ , \ \Phi_i = 3.34 D / L + 4.99 D / l_p \text{ and } \Phi_n = 4.486 D / L - 1.458 D / l_p \qquad (4)$$

To estimate the persistence length of our we use the formula[18] of mean square end-to-end distance $\langle h^2 \rangle$ for persistence chain model derived for short chains $L / l_p \ll 1$.

$$<h^2>=L^2\left[1-\frac{1}{3}\frac{L}{l_p}+\frac{1}{12}\left(\frac{L}{l_p}\right)^2\right] \qquad (5)$$

where $L=(N_c-1)l_o$ is the contour length of the chain. For our model we obtain the following persistent lengths in the systems considered: for $K_s=50$ $l_p=132$, for $K_s=100$ $l_p=199.7$, for $K_s=500$ $l_p=430.4$. The $<h^2>$ values corresponding to maximum density of isotropic phases of each system were used here.

By considering a molecule as a cylinder with diameter $D=\sigma$ and length $L=(N_c-1)\sigma$ we can determine the volume fraction of the polymer in our system $\Phi=\pi D^2L\rho/4N_c$. The values of the jump of order parameter $\Delta S$ and the volume fractions $\Phi_n$ were determined as corresponding values in the points on the curves in Figure 2, where curves remarkably change their slopes before the transition to the isotropic state. The values of $\Phi_i$ correspond to the points on these curves where their slopes change again at values of $S$ close to zero. A similar procedure was used to estimate these characteristics from the data, reported by Yethiraj and Fynewever[13] and Kolb[14].

In Figure 6 one can see that all values of $\Delta S$ determined from our, Kolb's or Yethiraj's and Fynewever's data for molecules with flexibility in a range considered in our study are in satisfactory agreement with theoretical predictions taking into account some uncertainty by fitting of parameters of the many particle models to the parameters of hard wormlike cylinder model and the accuracy of the theory[3].

To compare the values $\Phi_n$ and $\Phi_i$ for different models with theory predictions we use the reduced parameter $\Phi l_p/D$ [12]. In Figure 7 we see that for small $L/l_p$ (up to $\approx 0.1$) our and Kolb's data agree with theory predictions. For the more flexible molecules considered by Yethiraj and Fynewever and Kolb the values of boundary densities are lower than those following from formula 4. This disagreement could be expected because eq.4 are valid for $L/l_p \ll 1$. We do not analyse here the data, reported by Frenkel [12], because he considered mainly the region of larger values $L/l_p$ (from 0.1 to 10). This allows to conclude that the KS theory predictions for $\Delta S$, $\Phi_n$ and $\Phi_i$ agree rather well with existing simulation data for different models at $L/l_p \ll 1$.

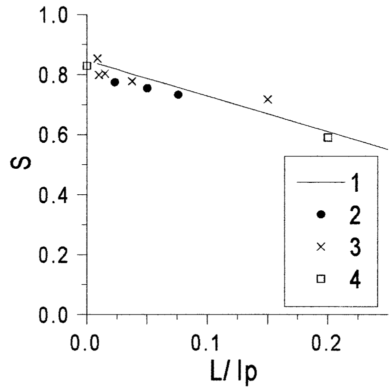

Figure 6. Order parameter $S$ at isotropic-nematic transition vs. ratio of chain length $L$ to its persistence length $l_p$ : 1- KS theory [5], 2- our simulation results, 3-Kolb[14] results, 4- Yethiraj and Fynewever[13] results.

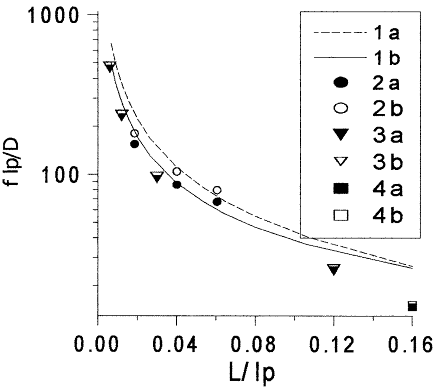

Figure 7. Scaled isotropic (I) and nematic (N) volume fractions at the phase transition vs. $L/l_p$: KS theory [5] (1a- I, 1b –N); our simulation results (2a- I, 2b –N); 3- Kolb[14] results (3a- I, 3b –N); 4- Yethiraj and Fynewever [13] results (4a- I, 4b –N).

## Dynamic Anisotropy

It is known that LC exhibits a dynamical anisotropy: the self- diffusion of molecules along the director is easier than that in the normal direction. The diffusion coefficients $D_{par}$ and $D_{per}$ were calculated from the slopes of mean square displacements. The dependences of diffusion coefficients $D_{par}$ and $D_{per}$ on the density for the most flexible ($K_s$ =50) and the most rigid ($K_s$ =500) of the systems considered can be seen in Figure 8 (a). In the crystal state the dynamics in both systems is very slow. As density decreases and the systems form the nematic LC phases the diffusion increases in both directions. At the same time the difference between diffusions in parallel and in perpendicular directions increase too. In the isotropic phase this difference disappears. The anisotropy of diffusion can be estimated from the ratio $D_{par}/D_{per}$. The ratio dependence on the density for the same systems as above is shown in Figure 8 (b). We do not observe any anisotropy in isotropic states, but found a very large anisotropy in the LC state. The more flexible system has the lower diffusion anisotropy: the maximum value of anisotropy is $D_{par}/D_{per}$ =3.3 for the system with $K_s$ =50 and $D_{par}/D_{per}$ =5.7 for the system with $K_s$ =500.

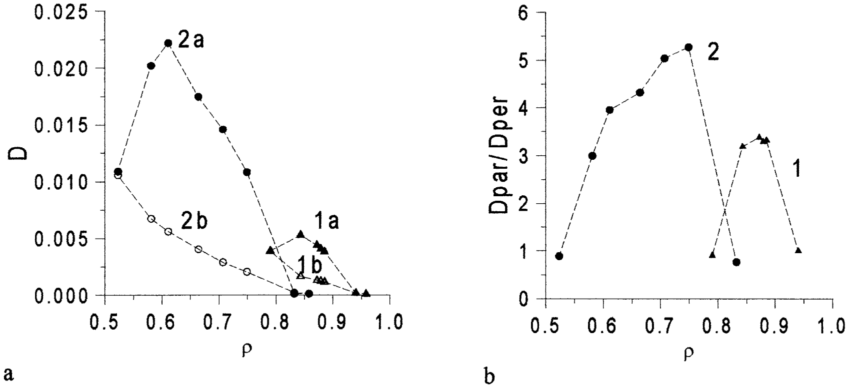

Figure 8. Diffusion coefficients (a) and anisotropy of diffusion (b) as function of density; ▲ = the system with $K_s$ =50: 1- $D_{par}$, 2- $D_{per}$, 5- $D_{par}/D_{per}$ ; • =the system with $K_s$ =500: 3- $D_{par}$, 4- $D_{per}$, 6 - $D_{par}/D_{per}$ .

### Semi-Flexible Polymer Brush

In a polymer brush the chains are anchored to the surface by one end. Due to the mutual repulsion chains became to be stretched [20-24] and height of brush increase $a^{1/3}$ with the increase of the grafting density $a$. Figure 9 shows the dependencies of the brush height $h_z$ and the component of gyration radius $R_{gz}$ normal to the surface on the grafting density obtained in our simulations. At moderate and intermediate density both for flexible and semi-flexible brushes these dependencies are in satisfactory agreement with theoretical predictions. At high densities there are some deviations from $a^{1/3}$ dependence in both cases. The theory also predicts [22] the increase of the height of the brush with the decrease of the chain flexibility as $l_p^{1/3}$ for semi-flexible chains. Because in our case the ratio of persistence lengths for two brushes is close to 4 (actually 3.8), the theoretical value for the ratio of their heights is near 1.56. Simulated values of this ratio change from 1.38 at moderate and intermdiate grafting densities to 1.18 at large $a$ (Table 1).

Due to the chain stretching in brush the order parameter $S$ grows with $a$ even for flexible chains. The theory (see for example[25]) predicts that the order parameter in brush increases gradualy with increase of polymer concentration in contrast to the step-like behaviour (LC phase transition) for semi-flexible polymer chains in solutions. Data in the Table 1 show that the order parameter for both brushes changes with the increase of grafting density in accordance with the theory.

Table 1.

| | Grafting density *a* | | | | | | | |
|---|---|---|---|---|---|---|---|---|
| | 0.007 | 0.025 | 0.050 | 0.075 | 0.100 | 0.200 | 0.300 | 0.400 |
| | Ratio of brush heights | | | | | | | |
| | 1.38 | 1.38 | 1.37 | 1.34 | 1.31 | 1.28 | 1.25 | 1.18 |
| | Order parameter *S* | | | | | | | |
| Flexible brush | 0.01 | 0.03 | 0.04 | 0.06 | 0.08 | 0.15 | 0.23 | 0.37 |
| Anisotropic brush | 0.05 | 0.09 | 0.12 | 0.16 | 0.20 | 0.36 | 0.51 | 0.71 |

More detailed information about the internal structure of brushes give the distribution function of monomers in Z direction (Figure 10) and distribution of free chain ends of the brush in the same direction (Figure 11). Both brushes show a similar behavior: the gradual transition from parabolic to box-like density profile and the shift of the chain ends to the brush periphery with increase of the grafting density .

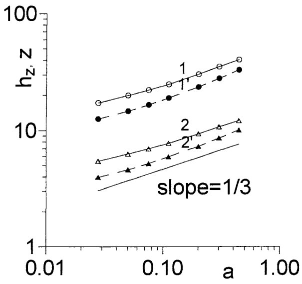

Figure 9. Hight of brush $h_z$ (1,1') and average hight of monomers *z* for anisotropic (semiflexible) brush (1,2) and flexible (1',2') brush.

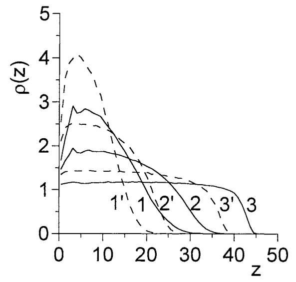

Figure 10. Distribution of density in the direction Z for semiflexible (solid lines 1-3) and flexible (dashed lines1'-3') brushes: (1,1') at a=0.03, (2,2') at a=0.1 and (3,3') at a=0.4

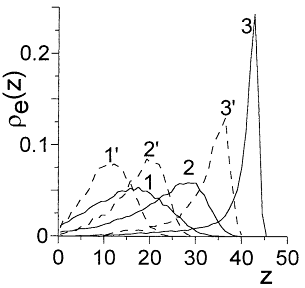

Figure 11. Distribution of chain ends in the direction Z for semiflexible (solid lines 1-3) and flexible (dashed lines1'-3') brushes: (1,1') at a=0.03, (2,2') at a=0.1 and (3,3') at a=0.4.

## Acknowledgement

We are very grateful to Professor M.P.Allen for helpful discussions. This paper is a part of the SUPERNET network research of European Science Foundation and INTAS project 99-1114. The financial support from the Academy of Finland and the Magnus Ehrnrooth foundation is gratefully acknowledged. Russian participants are grateful to the Russian Foundation of Basic Research (grants 99-03-33314 and 99-03-33404). Authors would like to express their gratitude to CSC for the computer time on Cray T3E and SGI Origin 2000.

[1] L. Onsager, *Ann. (N Y), Acad. Sci.* **1949**, *51*, 627.
[2] T. Odijk *Macromolecules* **1986**, *19*, 2313
[3] A.Yu. Grosberg, A.R. Khokhlov, *Soc. Sci. Rev. A Phys.* **1987**, *8*, 147.
[4] D. Frenkel, B.M. Mulder, *Mol. Phys.* **1985**, *55*, 1171
[5] A.R. Khokhlov, A.N. Semenov, *Physica A* **1981**, *108*, 546
[6] A.R. Khokhlov, A.N. Semenov, *Physica A* **1982**, *112*, 605
[7] H. Fynewever, A. Yethiraj, *J. Chem. Phys.* **1998**, *108*, 1636
[8] J.A. Veerman, D. Frenkel, *Phys. Rev. A* **1990**, *41*, 3237
[9] J.G. Gay, B.J. Berne, *J.Chem. phys.* **1981**, *74*, 33
[10] M.P. Allen, *Computer Phys. Commun.* **1999**, *121-122*, 219
[11] M.P. Allen, M.R. Wilson, *Molec. phys.* **1992**, *80*, 277
[12] M. Dijkstra, D. Frenkel, *Phys. Rev. E* **1995**, *51*, 5891
[13] A. Yethiraj, H. Fynewever, *Molecul. physics* **1998**, *93*, 693
[14]A.Kolb, Thesis, "Molekulardynamik-Untersuchungen zum Wechselspiel zwischen flussigkristalliner Ordnung und den Konformationen von Polymerketten, University of Mainz, 1999
[15] N. Balabaev, A. Darinskii, I. Neelov, A. Zarembo, F. Sundholm, *Polym. Sci.*, in press
[16] M.P. Allen, D.J. Tildsley, Computer Simulations of Liquids, Clarendon, Oxford 1987.
[17] H.J.C. Berendsen, J.P.M. Postma ,W.F. van Gunsterenm *J Chem Phys* **1984**, *81*, 3684.
[18] P. J. Flory, "Statistical Mechanics of Chain Molecules", Interscience Publishers, N.-Y., 1969.
[19] R. Hentschke, *Macromolecules* **1990**, *23*, 1192
[20] S. Alexander, *J.Phys.* **1977**, *38*, 983.
[21] P. De Gennes, *Macromolecules* **1980**, *13*, 1069; *Adv.Coll.&Int. Sci.* **1988,** *27*, 189.
[22] T. Birshtein, E. Zhulina, *Polymer. Sci.* (*USSR)* **1983**, *25*, 2165; *Polymer* **1984**, *25*, 1453.
[23] I. Neelov, K. Binder, *Macromol. Theory& Simul.* **1995**, *4*, 119; Ibid, **1995**, *4*, 1063.
[24] I. Neelov, O. Borisov, K. Binder, *Macromol. Chem. Theory Simul.* **1998**, 7, 141; *J.Chem.Phys.* **1998**, *108*, 6973.
[25] T.Birshtein, A. Mercurieva, L. Klushin, A. Polotsky, *Comput.Theor.Polym.Sci.* **1998**, *8*, 179.